Tissue Programmed Hydrogels Functionalized with GDNF Improve Human Neural Grafts in Parkinson's Disease

AUTHOR(S)

C P J Hunt, V Penna, C W Gantner, N Moriarty, Y Wang, S Franks, C M Ermine, I R de Luzy, C Pavan, B M Long, Richard Williams, L H Thompson, D R Nisbet, C L Parish

Tissue Programmed Hydrogels Functionalized with GDNF Improve Human Neural Grafts in Parkinson's Disease

Cameron P. J. Hunt, Vanessa Penna, Carlos W. Gantner, Niamh Moriarty, Yi Wang, Stephanie Franks, Charlotte M. Ermine, Isabelle R. de Luzy, Chiara Pavan, Benjamin M. Long, Richard J. Williams, Lachlan H. Thompson, David R. Nisbet,* and Clare L. Parish*

The survival and synaptic integration of transplanted dopaminergic (DA) progenitors are essential for ameliorating motor symptoms in Parkinson's disease (PD). Human pluripotent stem cell (hPSC)-derived DA progenitors are, however, exposed to numerous stressors prior to, and during, implantation that result in poor survival. Additionally, hPSC-derived grafts show inferior plasticity compared to fetal tissue grafts. These observations suggest that a more conducive host environment may improve graft outcomes. Here, tissue-specific support to DA progenitor grafts is provided with a fully characterized self-assembling peptide hydrogel. This biomimetic hydrogel matrix is programmed to support DA progenitors by i) including a laminin epitope within the matrix; and ii) shear encapsulating glial cell line-derived neurotrophic factor (GDNF) to ensure its sustained delivery. The biocompatible hydrogel biased a 51% increase in A9 neuron specification—a subpopulation of DA neurons critical for motor function. The sustained delivery of GDNF induced a 2.7-fold increase in DA neurons and enhanced graft plasticity, resulting in significant improvements in motor deficits at 6 months. These findings highlight the therapeutic benefit of stepwise customization of tissue-specific hydrogels to improve the physical and trophic support of human PSC-derived neural transplants, resulting in improved standardization, predictability and functional efficacy of grafts for PD.

1. Introduction

Clinical trials have provided proof of principle that the transplantation of new dopamine (DA) neurons into the striatum of Parkinson's disease (PD) patients can survive, integrate, and restore motor function.[1] Demonstrated using fetal tissue, these trials were hindered by challenges of standardization, ethics, and availability, and more recent efforts have focused on pluripotent stem cells (PSCs) as a viable source of DA neurons. Current differentiation protocols yield correctly specified ventral midbrain (VM) progenitors that, when implanted into animal models of PD, are capable of functionally integrating,[2] with similar efficacy to human fetal tissue.[3] These exciting observations have resulted in the recent commencement of, or plans for, multiple clinical trials.[4]

The number of DA neurons that survive in a graft is recognized as the most decisive factor in governing whether a transplant is successful in ameliorating symptoms, yet cell survival remains a major challenge for the field. Preclinical and clinical

C. P. J. Hunt, V. Penna, C. W. Gantner, N. Moriarty, C. M. Ermine, I. R. de Luzy, C. Pavan, L. H. Thompson, C. L. Parish
The Florey Institute of Neuroscience and Mental Health
The University of Melbourne
Parkville, VIC 3052, Australia
E-mail: clare.parish@florey.edu.au
Y. Wang, S. Franks, D. R. Nisbet
Laboratory of Advanced Biomaterials
Research School of Chemistry and the John Curtin School of Medical Research
The Australian National University
Canberra, ACT 2601, Australia
E-mail: david.nisbet@anu.edu.au

B. M. Long
School of Health and Life Sciences
Federation University
Mt Helen, VIC 3353, Australia
R. J. Williams
Centre for Molecular and Medical Research
School of Medicine
Deakin University
Waurn Ponds, VIC 3216, Australia
D. R. Nisbet
The Graeme Clark Institute, Faculty of Engineering and Information Technology & Faculty of Medicine
Dentistry and Health Services
The University of Melbourne
Melbourne, Australia

**ADVANCED
SCIENCE NEWS**

www.advancedsciencenews.com

**ADVANCED
FUNCTIONAL
MATERIALS**

www.afm-journal.de

studies report cell survival rates ranging from 1% to 20% for fetal tissue grafts,[5] and average dopamine neuron yields of <5% for human PSC-derived DA progenitor grafts.[2a,b,6] During transplantation cells undergo a series of physical traumas that render them susceptible to cell death, including detachment from underlying culture matrices, shear forces exerted during injection into the brain, and the adult host brain—an environment devoid of trophic cues.[5a,7]

Another decisive factor in the functional efficiency of these grafts is their capacity to integrate into existing host circuitry—specifically the synaptic connectivity of the A9 subpopulation of DA neurons in the graft with host striatal neurons.[8] While the requirement for this specific synaptic integration is known, the level of reinnervation of the host tissue by fetal-derived grafts remains well below that of the intact brain.[9] This is likely underpinned by the absence of trophic cues in the adult brain that are normally present during development. More recent studies have also highlighted suboptimal striatal innervation from human PSC-derived DA transplants, with these transplants displaying notably poorer plasticity when directly compared to human fetal tissue grafts.[3] Recognizing that the establishment of neural circuitry during development requires a tightly orchestrated physical and trophic environment suggests that greater attention to the host milieu may be required to promote survival, plasticity, and integration of human PSC-derived DA neurons.

A number of efforts to deliver trophic cues, aimed at influencing graft survival and plasticity, have been investigated. Surprisingly, however, little attention has been paid to the extracellular matrix (ECM) environment, despite its importance in providing both physical and chemical support for cells, including DA neurons.[10] Such insight presents new opportunities to engineer protective and cell-instructive microenvironments for neural grafts that can concomitantly act as programmable protein delivery vectors (see reviews in ref. [11]). Recently, we demonstrated that synthetic hydrogels functionalized with glial cell line-derived neurotrophic factor (GDNF—a potent inducer of DA survival and plasticity) could improve rodent fetal tissue grafting outcomes in models of PD.[12] In parallel work, we have shown peptide programmed hydrogels and advanced neural tissue-specific hydrogels could provide a sanctuary microenvironment for cells during implantation,[13] while additionally improving the survival, maturation, and functional integration of human PSC-derived neural grafts in models of stroke,[14] a response that could be enhanced through sustained delivery of a neurotrophic factor from the hydrogel.[15] Such observations raise the question whether similar neural tissue-specific biomaterials, functionalized with GDNF, may overcome many of the challenges currently hindering human PSC-derived VM progenitor grafts for PD.

We recently demonstrated that sustained GDNF (delivered in vivo via viral transduction of the host) can support hPSC-DA progenitor grafts.[16] However, unrestricted GDNF can impede DA graft plasticity, downregulate DA-associated genes, and/or impart effects on other neuronal populations in rodent and primate models.[16–17] Here, we show evidence that a neural tissue-specific laminin-based hydrogel is capable of controlled spatiotemporal GDNF release, that, in combination with DA progenitor transplantation, can ameliorate motor deficits in Par-

kinsonian rats. GDNF-loaded hydrogels modulated behavioral recovery through increasing DA survival, A9 specification, and graft plasticity. These findings highlight the potential therapeutic benefit of customized hydrogels to support human PSC-derived neural transplants in brain repair.

2. Experimental Section

2.1. Self-Assembled Peptide Hydrogel Fabrication

Self-assembling peptides (SAPs) were fabricated using solid phase peptide synthesis, as previously described.[18] Five peptides were created and screened to identify the optimal hydrogel sequence for supporting human PSC-derived VM progenitors. The peptide sequences, shown in **Figure 1**A, included: i) phenylalanine–phenylalanine (FF), ii) isoleucine–lysine–valine–alanine–valine (IKVAV), iii) lysine–isoleucine–valine–alanine–valine (KIVAV), iv) leucine–arginine–leucine–valine–leucine (LRLVL), and v) tyrosine–isoleucine–glycine–serine–arginine (YIGSR). To ensure self-assembly was spontaneous under physiological conditions, aspartate (D) or phenylalanine (F) residues were incorporated at the N-terminus of the peptide to modify the pKa of the molecule and thereby lower the pH at which spontaneous assembly occurred. Gelation was initiated using a well-established pH switch, as previously described, to yield a 20 mg mL^{-1} stock.[15] The final hydrogels were made by mixing at a 1:1 ratio with Hank's Balanced Salt Solution (HBSS) ± cells.

Following gelation, rheology was conducted to confirm a shear storage modulus, representative of stiffness, similar to the rat brain.[14,18] Fourier transform infrared (FTIR), circular dichroism (CD) spectroscopy, and transmission electron microscopy (TEM) verified synthesis and structure of the desired nanofibrillar structure for each of the peptide sequences,[18] which has been demonstrated to carry the functional epitope in a cell-accessible fashion on the surface of the assemblies. The resultant hydrogels could be reversed to an aqueous state by application of shear force (achieved via repeated titration or vortexing), such that the gel disassembled into a liquid solution. Reversal of the gel into a liquid state enabled incorporation and homogeneous distribution of GDNF recombinant protein into the polymer. This was referred to as incorporation of the functional protein into the polymer as shear encapsulation. Shear reversal of the gel also enabled incorporation of cells into the shear-thinned hydrogel for efficient dispersal and safe delivery into the brain.[15]

2.2. Assessment of Functional GDNF Release from SAP Hydrogel

To assess the release kinetics of GDNF from the scaffold, GDNF (100 ng, R&D Systems) was loaded into the SAP (50 µL) by reverse shearing of the gel to an aqueous state prior to casting the gel into a well of a 96-well plate. GDNF doses loaded into the hydrogel were based upon the previous work of prolonged neurotrophic factor release from gel-based scaffolds, including SAP.[12a,19] PBS (200 µL) was added to the well and incubated at 37 °C. The supernatant was collected at numerous intervals over a 4-week period. All supernatant samples were
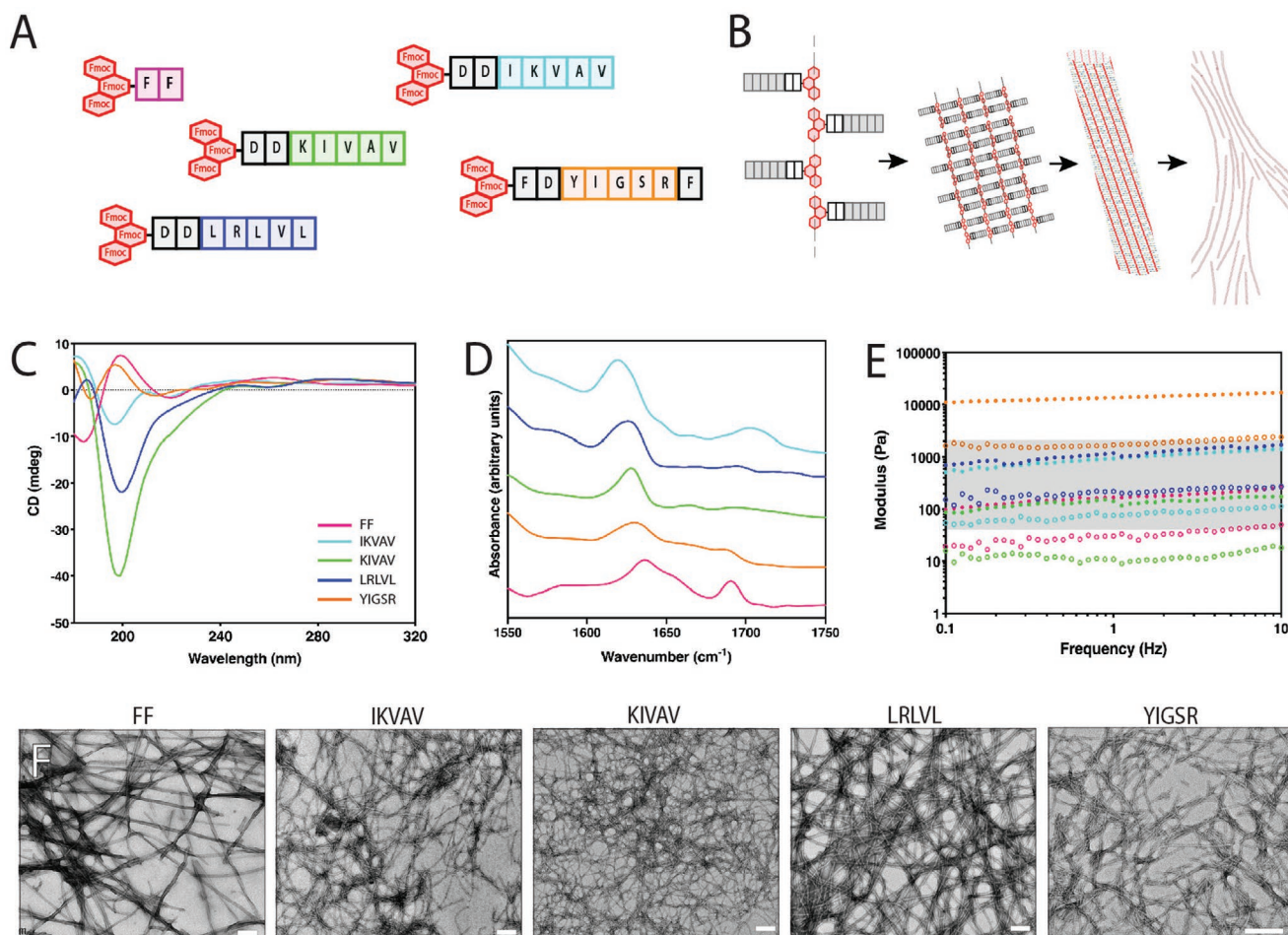
**ADVANCED
SCIENCE NEWS**

www.advancedsciencenews.com

**ADVANCED
FUNCTIONAL
MATERIALS**

www.afm-journal.de

Figure 1. Generation of SAP hydrogel biomaterials. A) Illustration of the five different Fmoc-based peptide sequences. B) Schematic peptide structure showing its self-assembly, leading to a natural nanofibrillar structure (combination of amphiphilic organization, π–π interactions, and the β sheet folding forming the nanofibrils). C) The stable formation of a dominant assembly, confirmed by circular dichroism spectroscopy, showing transition peaks at 200–220 nm for the five different peptides. D) Peptide interaction, through hydrogen bonds forming and secondary β sheets was confirmed for the five different peptides by Fourier transform infrared (FTIR) of amide I region, showing characteristic peak for β sheets with an observable carbamate peak. E) Storage (filled circles) and loss (open circles) modulus for the five different peptide-based hydrogels, showing similar stiffness to the rodent brain (indicated by gray shading). F) Representative electron micrographs for the five peptide-based hydrogels illustrating the appropriate assembly of the nanofibrils. Scale bars: F) 100 nm.

immediately stored at −20 °C until the time of analysis. The GDNF levels (protein unfolding and cumulative release) were quantified by enzyme linked immunosorbent assay (ELISA), using previously described methods.[12a,20] Release profiles were performed in triplicate wells for each time point and repeated on three independent experiments.

Small angle X-ray scattering (SAXS) was performed using the beamline at the Australian Synchrotron. Hydrogel samples were prepared, as per above, two days before testing and stored in Eppendorf vials. Immediately prior to exposure, PBS (containing recombinant GDNF protein) backgrounds were loaded into 1.5 mm glass capillaries with 0.1 mm wall thickness. Backgrounds were measured in triplicate with ten 1 s exposures at multiple offset locations to avoid radiation damage. Two SAP samples containing GDNF were measured in triplicate using the same protocol, however, the SAP samples were loaded 24 h prior to exposure to allow ample time for reassembly.

Measurements were conducted at two different camera lengths: 900 and 7000 mm to capture a q-range between 0.007 and 1 Å^{-1}. Data reduction was performed using ScatterBrain, with averages taken for each sample on each camera length and relevant backgrounds subtracted. Data for each sample for the two different camera lengths were then combined using Microsoft Excel, analyzed using $P(r)$ inversion, and subjected to a power law analysis using SASView.

The functionality of the GDNF released from the hydrogels was confirmed using previously described methods.[15] As described above, GDNF was shear-encapsulated into SAP, cast into a 48-well plate, and 100 μL of media was added. Conditioned media (shGDNF-CM) was collected after 12 h and applied to primary ventral midbrain neurons for comparison to untreated cultures as well as those treated directly with recombinant GDNF protein (soluble GDNF (sGDNF) 20 ng mL^{-1}). Primary VM cultures were performed and assayed as previously

**ADVANCED
SCIENCE NEWS**
www.advancedsciencenews.com

**ADVANCED
FUNCTIONAL
MATERIALS**
www.afm-journal.de

described.[21] In brief, VM tissue was microdissected from the brains of embryonic day 11.5 (E11.5) embryos that were obtained from time-mated mice expressing GFP under the tyrosine hydroxylase promotor. VM tissue was dissociated using 0.05% trypsin and 0.1% DNase, subsequently blocked using 10% serum, and the cells resuspended in N2 media. Cells were seeded at a density of 125 000 cells per well in 48-well plates (coated with PDL/laminin). After 72 h, cultures were fixed with 4% paraformaldehyde and TH+ neuron number and neurite length were assessed.

2.3. Ventral Midbrain Specification of Human Pluripotent Stem Cells

The H9 human embryonic stem cell (hESC) reporter line expressing eGFP under the *LMX1A* promotor (LMX1A-eGFP) was expanded and differentiated to a ventral midbrain progenitor identity as previously described.[2c] In brief, the cell line, confirmed to be karyotypically normal and routinely tested for the absence of mycoplasma, was cultured on laminin 521 (BioLamina) in mTeSR1 (StemCell Technologies) supplemented with 0.5% penicillin–streptomycin (Life Technologies). To promote neural induction, cells were exposed to dual SMAD inhibition using LDN193189 (200×10^{-9} M, Stemgent; from 0 to 11 days in vitro (DIV)) and SB431532 (10×10^{-6} M, R&D Systems; 0–5 DIV). Ventral patterning was achieved by addition of sonic hedgehog (C25II, 100 ng mL^{-1}, R&D Systems; 1–7 DIV) and purmorphamine (2×10^{-6} M, Stemgent; 1–7 DIV), and the cells caudalized to a midbrain identity by Wnt activation using CHIR99021 (3×10^{-6} M, Miltenyi Biotech; 3–13 DIV). Cells were maintained in culture from 13 DIV in media supplemented with BDNF (20 ng mL^{-1}, R&D Systems), GDNF (20 ng mL^{-1}, R&D Systems), ascorbic acid (200×10^{-9} M, Sigma-Aldrich), and TGF3β (1 ng mL^{-1}, PeproTech), cAMP (0.05×10^{-3} M, Tocris), and the notch inhibitor DAPT (10×10^{-6} M, Sigma-Aldrich). Regional identity of the differentiating cells was verified at 11 DIV by immunohistochemistry. In preparation for grafting, at 19 DIV cultures were dissociated using Accutase (Life Technologies) and correctly specified ventral midbrain progenitors isolated by fluorescent activated cell sorting (FACS) based upon expression of LMX1A-eGFP, using previously described methods.[22]

The functionality of the GDNF released from the hydrogels was additionally confirmed on human cultures. As hPSC-derived VM progenitors were routinely matured in the presence of GDNF, cultures were compared in the presence and absence of soluble GDNF (20 ng mL^{-1}, R&D Systems) to cultures in which the media was supplemented with 10% conditioned media (shGDNF-CM). Cultures were treated from day 13 to day 26 and assessed at 26 DIV for viability and the proportion of TH+ DA neurons.

2.4. Surgical Procedures

All animal procedures were conducted in agreement with the Australian National Health and Medical Research Council's published Code of Practice for the Use of Animals in Research,

and experiments approved by The Florey Institute of Neuroscience and Mental Health Animal Ethics committee. Animals were group housed in individually ventilated cages with low irritant bedding on a 12:12 h light/dark cycle with ad libitum access to food and water. Surgeries were performed on 75 athymic nude mice (*Foxn1*nu/Arc) and 55 athymic (CBHrnu) nude rats under 2% isofluorane anesthesia, as previously described.[16] Rats received unilateral 6-OHDA (3.5 μL, 3.2 μg μL^{-1}) lesions of the medial forebrain bundle at the following stereotaxic coordinates: 3.4 mm caudal, 1.4 mm lateral to bregma, and 6.8 mm below the surface of the dura. 6OHDA (1.6 μL, 1.5 μg μL^{-1}) was injected directly into the substantia nigra (SN) within the ventral midbrain of mice at 3.0 mm posterior, 2.0 mm lateral to bregma, and 4.0 mm below the surface of the brain.

At 4 weeks after 6-OHDA lesioning, human ESC-derived LMX1A-eGFP expressing VM progenitors (with or without the SAP hydrogel) were transplanted into the denervated striatum (100 000 cells in 2 μL) at the following coordinates in rats (and mice): 0.5 mm (1.0 mm) anterior, 2.5 mm (2.0 mm) lateral to Bregma, and 4.0 mm (2.8 mm) below dura. Treatment groups were as follows for short-term (6 weeks) graft survival: Cells only, Cells + FF, Cells + IKVAV, Cells + KIVAV, Cells + LRLVL, and Cells + YIGSR. For long-term graft survival in Parkinsonian rodent models, groups included: Lesion, Lesion + LMX1A-eGFP + VM progenitors (subsequently referred to as "Cells"), Lesion + Cells + DDIKVAV SAP (referred to as "Cells + SAP"), Lesion + Cells + soluble GDNF ("Cells + sGDNF"), and Lesion + Cells + SAP shear-encapsulated with GDNF (Cells + SAP-shGDNF). Group sizes were $n = 5–6$ mice for short-term histological assessment of grafts at 6 weeks, $n = 6–7$ rats per group for long-term behavior and histology, $n = 5–6$ mice per group for high performance liquid chromatography (HPLC), and $n = 5$ mice per group for transcriptional profiling of the grafts.

Recombinant GDNF protein was delivered in vivo (mixed with cells or shear-encapsulated into the IKVAV polymer) at a final concentration of 1 μg per injection, in accordance to previously adopted GDNF doses employed for alternate hydrogels in the support of rodent fetal grafts.[12a] A total of 100 000 cells were injected per animal, delivered within the SAP hydrogel (at a final concentration of 10 mg mL^{-1}) or HBSS media. All animals received a final injection volume of 2 μL.

2.5. Behavioral Testing

Behavioral assessment of motor impairment was performed 3 weeks after unilateral 6-OHDA lesioning using the amphetamine-induced rotation and cylinder tests, as previously described.[16] In brief, for rotational testing, net rotations over 60 min were analyzed 10 min after intraperitoneal injection of D-amphetamine sulfate (5 mg kg^{-1}; Tocris Bioscience). Animals displaying a functional deficit (>300 rotations h^{-1}), indicative of extensive unilateral ablation of the midbrain dopamine pathway, were included in the study. The 33 rats reaching criteria were ranked in order of the percentage rotational asymmetry and evenly distributed across the 5 treatment groups. For the cylinder test, rats were placed within a clear glass cylinder and the first 20 forepaw touches were recorded over three consecutive days. Data were presented as left paw ratio

ADVANCED
SCIENCE NEWS
www.advancedsciencenews.com

ADVANCED
FUNCTIONAL
MATERIALS
www.afm-journal.de

(Left/(Left + Right)) × 100. Rotational testing was repeated at 16, 20, and 24 weeks and the cylinder task at 24 weeks post-transplantation. Note that the delivery of GDNF or SAP into 6-OHDA lesioned rats, in the absence of cell grafts, had no impact on motor performance, with stable motor deficits observed at 24 weeks, indistinguishable from Lesion only animals (data not shown). Beyond motor assessment, these animals were not further analyzed in the present study. All experimenters were blinded to the treatment groups at the time of behavioral testing.

2.6. Tissue Processing and Immunohistochemistry

At 24 weeks postimplantation, all animals received an acute injection of D-amphetamine sulfate (5 mg kg^{-1}) prior to an overdose of sodium pentobarbitone (100 mg kg^{-1}). Animals were transcardially perfused with 4% paraformaldehyde and the brains processed for immunohistochemistry as previously described.[14] Primary antibodies and dilution factors were as follows: mouse anti-CD11b (1:100, Serotec), goat anti-cFOS (1:1000, Santa Cruz), goat anti-FOXA2 (1:200, Santa Cruz), rabbit anti-GFAP (1:200, DAKO), chicken anti-GFP (1:1000; Abcam), rabbit anti-GFP (1:20000; Abcam), mouse anti-human nuclear antigen (HNA, 1:300, Millipore), mouse anti PSA-NCAM (1:200, Santa Cruz), mouse anti-Nestin (1:200, Millipore), mouse anti-NeuN (1:100; R&D Systems), rabbit anti-OTX2 (1:4000; Millipore), mouse anti-synaptophysin (1:1000, human specific, Enzo Life Sciences), anti-rat endothelial cell antigen-1 (RECA-1, 1:500, Serotec), rabbit anti-tyrosine hydroxylase (TH) (1:500, Pel-Freeze), and sheep anti-TH (1:800, Pel-freeze). Secondary antibodies for i) direct detection were used at a dilution of 1:200—DyLight 488, 550/594, or 649 conjugated donkey antimouse, antichicken, or antirabbit (Jackson ImmunoResearch); and ii) indirect with streptavidin–biotin amplification—biotin conjugated donkey antirabbit (1:500; Jackson ImmunoResearch) followed by peroxidase conjugated streptavidin (Vectastain ABC kit, Vector laboratories), or 649 conjugated streptavidin (1:200; Jackson ImmunoResearch). Total cells in vitro and in vivo were visualized with 4′,6-diamidino-2-phenylindole (DAPI, 1:5000, Sigma-Aldrich). All fluorescent images were captured using a Zeiss Axio Observer Z1 epifluorescence or Zeiss confocal microscope system. Bright- and dark-field images were obtained using a Leica DM6000 upright microscope.

Total number of HNA+, TH+, GIRK2+, CALBINDIN+, as well as density of NeuN+ and cFOS+ cells were counted from images captured at 20× magnification. The density of graft-derived PSA-NCAM labeling (% immunoreactive pixels) within the dorsolateral striatum (the midbrain DA forebrain target that underpins gross motor function) was assessed from images captured at 20× magnification and analyzed using ImageJ software. Density of human specific synaptophysin (hSYP; expressed as % immunoreactive voxels) as well as %TH+ puncta coexpressing hSYP (indicative of graft-derived DA synapses) was assessed from confocal captured images at 40× and analyzed using iMaris software (Bitplane, USA).

The immunological response of the host brain to the implantation of the cells and/or the SAP scaffold (including the presence of GDNF) was assessed at predetermined sites lateral to the graft-host border (delineated according to GFP labeling), as depicted in Figure S2A in the Supporting Information. The area covered by GFAP or CD11b immunoreactivity was expressed as a percentage of the total pixels, as previously described.[23] RECA-1+ and CD34+ immunostaining was employed to identify specific host and host + graft-derived blood vessels within the graft and host tissue. Vessel density (expressed as the percentage total area covered by staining), within graft and host tissue, was estimated using previously described methods.[14]

2.7. High Performance Liquid Chromatography

Using previously described methods,[24] reverse phase liquid chromatography with electrochemical detection was employed to measure dopamine levels in the striatum of mice at 6 months after the transplantation of hPSC-derived VM progenitors (±SAP ± GDNF). Data were expressed as the percentage of dopamine relative to the intact/unlesioned striatum.

2.8. Transcriptional Profiling

For transcriptional profiling, striatal tissue containing the hPSC-derived VM progenitor transplants (Cells and Cells + SAP-shGDNF) was dissected from mice. Total RNA was extracted and qRT-PCR performed as previously described.[25] To selectively assess these gene expression changes in the graft (human origin) and not host tissue (mouse), qPCR primers were designed against regions containing little sequence homology between the human and mouse gene. Primers were validated for their selectivity on control mouse (no expression) and human (gene expression) tissue, prior to testing on grafted samples. See **Table 1** for a list of primers.

2.9. Statistical Analysis

All data were presented as mean ± SEM. Statistical tests employed's (inclusive of one-way ANOVA and Student's *t*-tests) are stated in the figure legends. Alpha levels of $p < 0.05$ were considered significant with all statistical analysis performed using GraphPad Prism Software, v 9.01, La Jolla, CA, USA. $^{*}p < 0.05$, $^{**}p < 0.01$, $^{***}p < 0.001$, and $^{****}p < 0.0001$.

3. Results

3.1. Fabrication of Peptide-Based Scaffolds to Mimic the Brains Extracellular Matrix Properties

The current study examined the capacity of a GDNF-functionalized hydrogel to support human pluripotent stem cell-derived VM progenitor grafts in a rat model of Parkinson's disease. To achieve this, we examined a series of peptides of varying lengths and amino acid sequences—with both unknown and known functionality. The peptide sequences examined

Table 1. List of primers used for QPCR.

Gene symbol	Gene name	Primer (forward)	Primer (reverse)
PSMB4	House Keeping Gene (HKG)	TGCACTTTACAGAGGTCCAATC	CGTAGGATCCCAGCATGTCT
Nestin	Nestin	AGCGTTGGAACAGAGGTTG	GCCAACCAGATAACATGTTAACA
SYT12	Synaptotagmin 12	CTGTCTGATGCCCTCTCCAT	CACTCCTCTGCTGCAATCTG
LMX1A	LIM Homeobox Transcription Factor 1 Alpha	ATGAACCCCTACACGGCTCT	TAAGGGTGCATGTGGTCTCC
EN1	Engrailed-1	AAGAAATAGCCAAGTGTCTCCA	GTCTGGCCTGGATCGCTC
TH	Tyrosine hydroxylase	GAGGCCATCATGGTAAGAGGG	CTGCCTGCGCCCAATGAAC
GIRK2	G-protein-regulated inward-rectifier potassium channel 2	TGCGGATTTCATGACGTCTC	TGGAATGAAGTGGGGAAAGATAA
D2R	Dopamine D2 receptor	AGCAAGCTCTCTTGCCGAGG	TGAGGTGGGTCCGGACTAGCC
DAT	Dopamine Transporter	TTCCTCAACTCCCAGTGTGC	CCGTTCTGCTCCTTGACAAG
VMAT2	Vesicular monoamine transporter 2	ACAGCTAGTTCTCTCAAGTGTAG	GCCAACCAGATAACATGTTAACA

included: i) FF, one of the simplest, nonfunctional dipeptides that is capable of forming nanotubes upon self-assembly; ii) IKVAV, a fragment of the binding domain of the α1 chain of the ECM protein laminin that is known for its critical roles in cell attachment, proliferation, differentiation, and plasticity,[26] and has previously been shown by us to support the integration of human PSC-derived cortical grafts in stroke models;[14–15] iii) KIVAV, the scrambled IKVAV sequence that would enable assessment of the importance of the specific amino acids and their sequence; iv) LRLVL, a peptide of comparable size consisting of amino acids with similar properties (i.e., charge, polar/nonpolar, hydrophobic/philic) to the IKVAV sequence to further assess the importance of select amino acid residues; and v) YIGSR—an alternate laminin epitope (of the β1 chain).

Upon self-assembly, these amino acid-based hydrogels were predicted to mimic structural attributes of the brain's native ECM, while IKVAV and YIGSR would provide additional laminin-associated functional properties. To enable assembly under physiological conditions (pH 7.4), aspartate or phenylalanine residue(s) were added to the N-terminus of the peptides (and C-terminus of the YIGSR peptide) to adjust the pKa, resulting in the final peptide sequences FF, DDIKVAV, DDKIVAV, DDLRLVL, and FDYIGSRF (Figure 1A).

In the fabrication of the peptides, aromatic N-fluorenylmethloxy carbonyl (Fmoc) moieties were used to protect the amino-terminus, which during self-assembly also promote stability via π–π interactions, creating the backbone structure (shown in red in Figure 1B). These individual peptides interacted through hydrogen bonds to form secondary β-sheets that were confirmed by CD (Figure 1C) and FTIR spectroscopies (amide peak at 1620 cm^{-1}) (Figure 1D). Through a combination of amphiphilic organization, π–π interactions, and the β sheet motifs, extended networks of nanofibrils were formed. These nanofibrils interacted to create hydrated bundles (Figure 1B), forming the matrix of the hydrogel, and could be visualized by TEM (Figure 1F). The individual nanotubes formed by each of the five peptide sequences were not significantly different in size (data not shown) and displayed comparable random organization (Figure 1F). Appropriate for in vivo delivery and the support of implanted neural progenitors, the resultant gels (at 10 mg mL^{-1}) had a storage (G') and loss (G'') modulus similar to the rat brain (ranging from 0.3 to 1.1 kPa,[27] gray shading) (Figure 1E).

3.2. Identification of Optimal SAP Hydrogels to Support the Survival of Transplanted Neural Progenitors and Modulate Local Inflammation

Next, we assessed the ability of each of the SAP hydrogels to support the survival of human PSC-derived VM neural progenitor grafts—the cell population required to replace dopamine neurons that progressively degenerate in Parkinson's disease. The progenitors were differentiated from LMX1A-eGFP human pluripotent stem cells using an established xenogeneic-free protocol.[2c] Appropriate and efficient VM fate specification of the cells in culture was validated at day 11 of differentiation (D11) by the coexpression of floorplate marker FOXA2, forebrain-midbrain transcription factor OTX2, and neural progenitor marker NESTIN—coexpressed in >85% of cells (**Figure 2**A,B). At the time of transplantation (19 DIV), 77.5% of cells expressed the early intrinsic dopamine determinant transgene LIM homeobox transcription factor 1α (LMX1A-eGFP+; Figure 2C). This population could be readily isolated by FACS (Figure 2D), for the purpose of VMDA neuron enrichment in grafts, as previously described.[22]

Isolated VM progenitors were transplanted into the brain of immune compromised athymic mice. After 6 weeks, viable grafts were observed within the striatum of 29 out of the 30 mice, detected by immunolabeling against the protein for HNA (Figure 2E). Only grafts supported by the IKVAV SAP hydrogel showed comparable graft volume and cell numbers to transplants of Cells only (Figure 2F,G), and were without elevated GFAP+ reactive astrocyte levels (Figure 2H,I). Such observations suggest that further study into region-specific ECM differences may aid design of future hydrogels for targeted, regional specific tissue repair α1 subunit epitope (IKVAV) and not merely the presence of the peptide-based hydrogel—noting that nonfunctional SAP gels (of similar and smaller size including LRLVL and FF) as well as the scrambled IKVAV sequence (KIVAV). Furthermore, an alternative functional laminin epitope (YIGSR, of the β1 subunit) failed to yield comparable grafting outcomes. Consequently, the IKVAV SAP hydrogel was employed for subsequent functionalization with GDNF and assessment of long-term grafting outcomes in rodent models of Parkinson's disease.
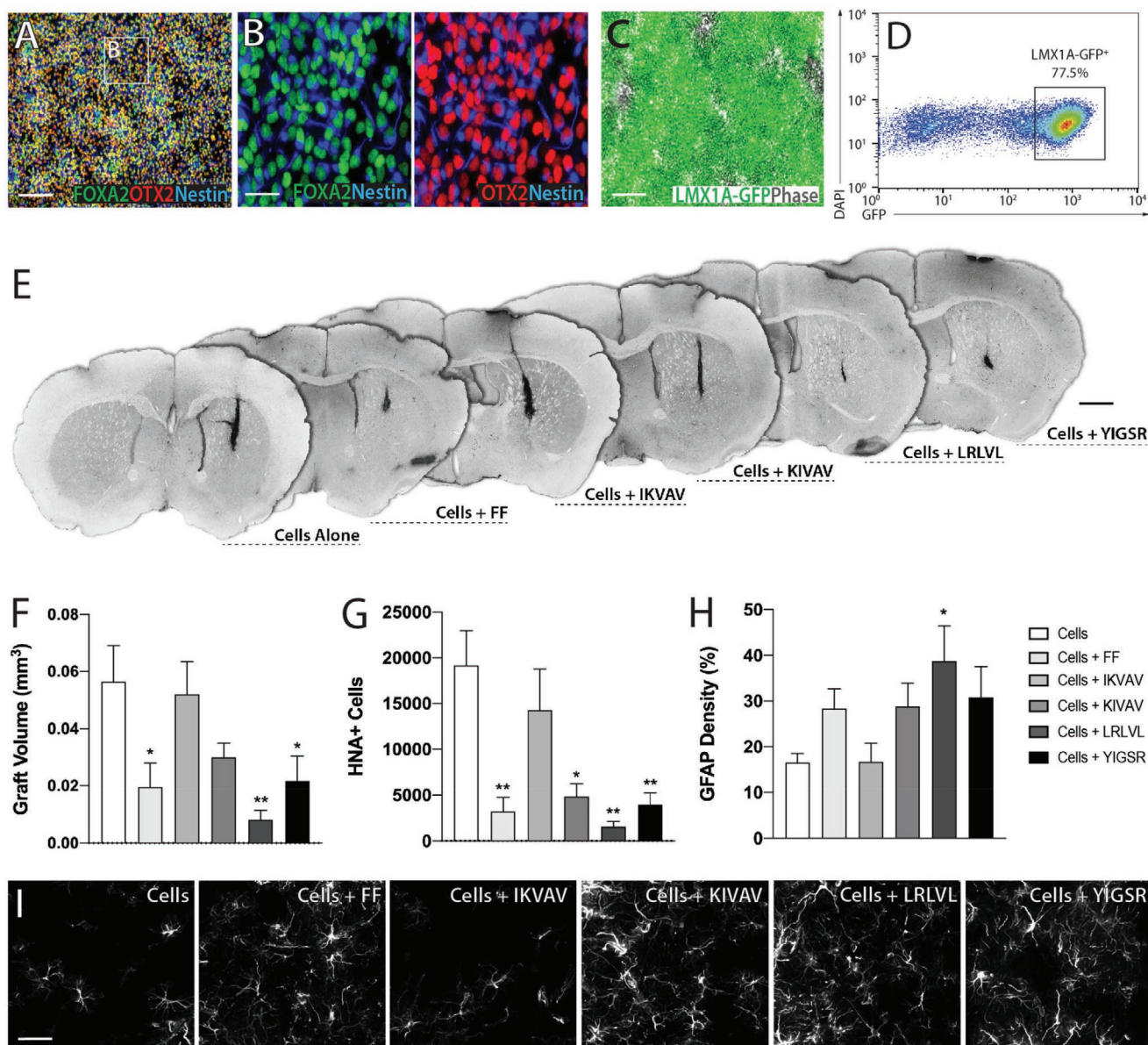
Figure 2. Differentiation of hPSC-derived VM progenitors suitable for coimplantation and screening of the peptide-based SAP hydrogels. A,B) VM fate specification of human PSCs at 11 DIV was confirmed by the coexpression of FOXA2, OTX2, and NESTIN. C) Expression of the early intrinsic determinant transgene, LMX1A, at the time of transplantation (21 DIV). D) Use of an LMX1A-eGFP reporter human PSC cell line enabled isolation of correctly specified VM progenitors, by FACS, prior to transplantation. E) Representative photomicrographs illustrating the hPSC-derived VM progenitor grafts in the absence and presence of the 5 SAP hydrogels, 6 weeks after implantation. F) Quantification of the volume and G) number of human nuclear antigen (HNA+) cells within the grafts (+various SAP hydrogels). H) Density of GFAP+ astrocytes (% immunoreactive pixels) surrounding the SAP-supported cell grafts. Note that only cell grafts in the presence of the IKVAV SAP hydrogel showed comparable size and cell number to grafts of Cells alone, without enhancing local inflammation. Data represent mean ± SEM. A–D) Representative of three independent cultures; E–I) $n = 5$ grafts per group. $^*p < 0.05$ and $^{**}p < 0.01$, showing significant difference from grafts of Cells alone. Scale bars: A,C) 200 μm, B) 50 μm, E) 1 mm, and I) 100 μm.

3.3. Tissue-Specific Scaffolds Deliver Functional GDNF to Promote DA Survival and Plasticity In Vitro

Next, we assessed the ability of the IKVAV SAP hydrogel to sustain delivery of GDNF over extended time frames and influence the behavior of both rodent and human VM progenitors in vitro. Importantly, shear encapsulation of the SAP hydrogel with GDNF had no impact on the assembly or mechanical prop-

erties of the gels (**Figure 3**A–D). The structure of the IKVAV hydrogel and the hydrogel loaded with GDNF were further examined using SAXS. The X-ray scattering profiles revealed no significant differences between the IKVAV SAP (Gel) and the GDNF-loaded SAP (Gel + GDNF) (Figure 3E). Scattering from the nanofibrils was consistent with a cylindrical-like structure (q^{-1} relationship at low q) with a diameter of 12.6 nm ± 0.9 nm. The profile and diameter of the SAP with GDNF was consistent

**ADVANCED
SCIENCE NEWS**

www.advancedsciencenews.com

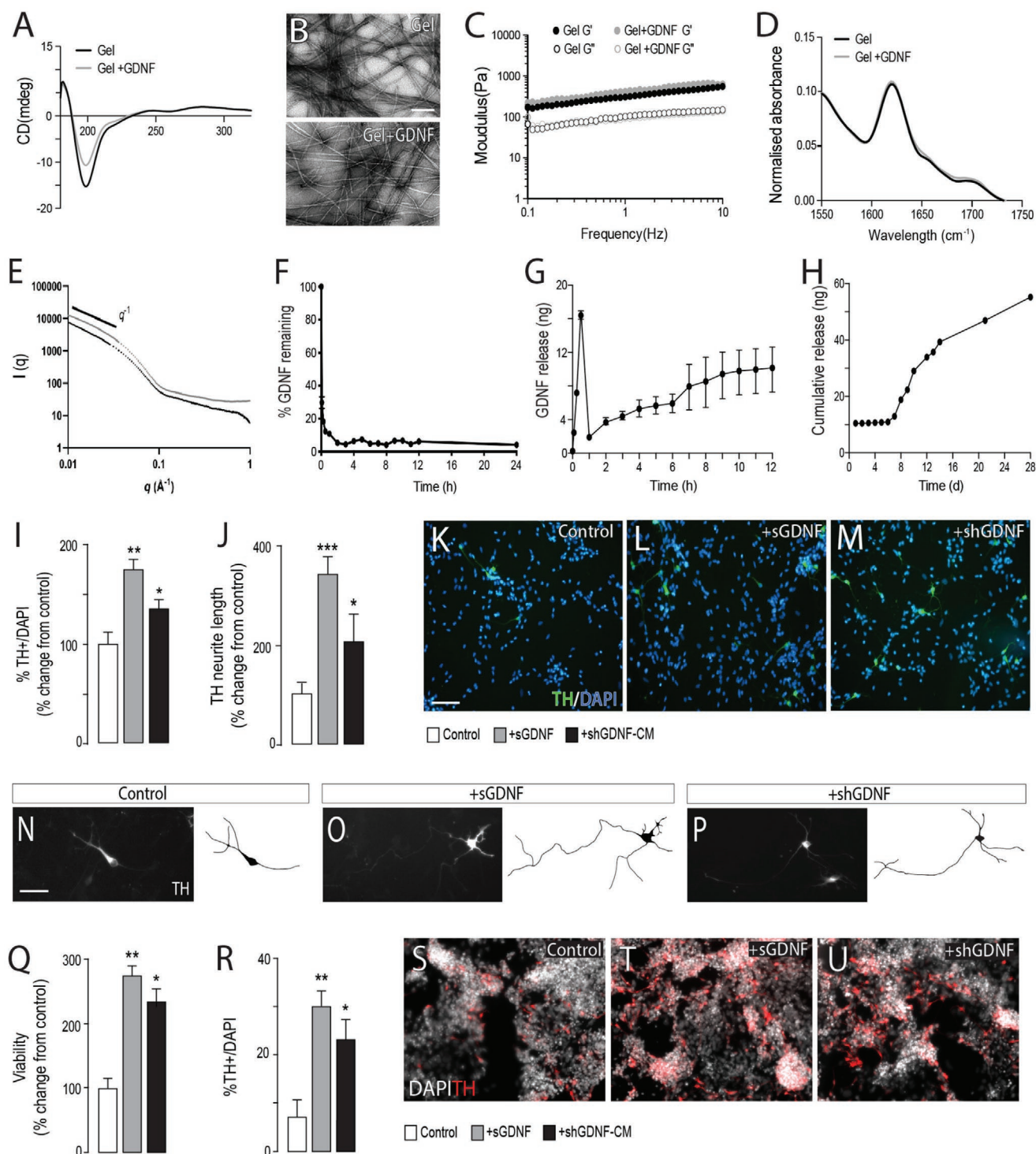**ADVANCED
FUNCTIONAL
MATERIALS**

www.afm-journal.de

Figure 3. Delivery of GDNF from IKVAV SAP hydrogels and confirmation of maintained functional activity. A) The shear encapsulation of GDNF had no impact on the physical properties of the IKVAV hydrogel with circular dichroism spectroscopy confirming a maintained stable formation of a dominant assembly, B) electron microscopy showing sustained nanofibrils structure, and C) rheology validating retained storage and loss modulus properties for the functionalized gel. D) X-ray scattering profiles revealed no significant differences between the Fmoc-DDIKVAV SAP (Gel) and the GDNF-loaded SAP (Gel + GDNF), indicating that incorporation of the recombinant protein into the gel did not adversely affect the structural mechanism driving scaffold formation. E) FTIR confirmation that GDNF encapsulation did not alter scaffold structure. F) Soluble GDNF in media was rapidly degraded (>90% degradation within 2 h). G,H) Shear entrapment of GDNF within the hydrogel resulted in an initial burst release (within 15 min), followed by a delayed and sustained release, observed over 28 days. I,J) VM primary cultures treated with soluble recombinant GDNF protein (sGDNF) and with conditioned media collected from SAP hydrogels shear loaded with GDNF (shGDNF-CM), confirming GDNF functionality—as revealed by increased

with the SAP alone (diameter of 12.8 nm). The unchanged scattering profile indicates that incorporation of the GDNF recombinant protein into the gel did not adversely affect the structural mechanism that drives formation of the scaffold.

Importantly, we confirmed the stability and functionality of GDNF released from the SAP hydrogels in vitro, prior to in vivo delivery. Surprisingly, recombinant GDNF protein added directly to the culture media, rapidly unfolded/degraded, with just 20% of the protein present after 15 min, and less than 3% at 24 h (Figure 3F). In contrast, shear encapsulation of the protein within the hydrogel resulted in an initial burst release within the first 15 min, likely the consequence of poorly entrapped GDNF rapidly leaking from the hydrogel prior to reforming, which was followed by a delayed and sustained release from 7 to 14 days (Figure 3G,H). To confirm the functionality of the GDNF protein released from the SAP hydrogels, prior to in vivo testing, we treated VM primary cultures, isolated from the developing mouse embryo and rich in DA progenitors, with soluble recombinant GDNF protein (sGDNF) or conditioned media collected from GDNF shear-encapsulated SAP gels (shGDNF-CM). As anticipated, sGDNF treatment resulted in a significant increase in the survival of TH+ DA neurons in culture (%TH+/DAPI; Figure 3I,K,L), as well as TH+ neurite length (Figure 3J,N,O), effects that were mimicked by treatment of the cultures with shGDNF-CM (Figure 3I,J,M,P). The maturation of human PSC-derived VM progenitors into TH+ DA neurons is dependent on the inclusion of GDNF within the daily supplemented media.[28] Consequently, while omission of GDNF from the media resulted in poor cultures (Control), daily supplementation of the media from day 13 to day 26 of differentiation with shGDNF-CM resulted in increased viability and proportions of TH+ DA neurons, comparable to those treated with sGDNF (Figure 3Q–U).

3.4. GDNF-Functionalized Scaffolds Promote Functional Recovery and Increased Graft Survival in Parkinsonian Rats

GDNF shear-encapsulated IKVAV SAP hydrogels were subsequently tested for their capacity to support the long-term structural and functional integration of hPSC-derived VM progenitor grafts in the Parkinsonian rat brain (**Figure 4**A). Behavioral testing, for asymmetric motor dysfunction in unilaterally 6OHDA lesioned rats, was performed 4 weeks after 6OHDA lesioning (pretransplantation, Pre-Tx) and repeated at 24 weeks after grafting (Figure 4B). All animals displayed rotational asymmetry (>6 rotations min^{-1}) prior to grafting, a deficit that only persisted in ungrafted animals (Lesion only) at 24 weeks (Figure 4C). By 20 weeks only animals receiving grafts in the presence of the GDNF-functionalized IKVAV SAP hydrogel showed a significant reduction in rotations (Figure S1, Supporting Information). As previously reported by us and others,[2–3,6a,16,22,29] by 6 months, the hPSC-derived VM progenitor grafts (irrespective of the presence of the hydrogel and/

or GDNF) were capable of reversing the amphetamine-induced motor asymmetry (Figure 4C). This correction of rotational behavior across all grafted groups reflects the low threshold number of DA neurons (combined with the amphetamine-induced release of their dopamine) that has been reported to be required, to improve this motor deficit.[3,30] More challenging for the field remains the ability to reverse sensorimotor deficits using nonpharmacologically induced tests. In the cylinder task, used to assess spontaneous motor function, all animals prior to transplantation showed a deficit in the contralateral forepaw use (≈10% use of the impaired contralateral, compared to the unimpaired ipsilateral paw). Only animals receiving grafts in the presence of GDNF-functionalized SAP scaffold (Cells + SAP-shGDNF; black bars) showed a significant improvement in limb use 24 weeks after grafting (Figure 4D).

In support of the observed improvement in rotational asymmetry, 24 weeks after transplantation, all animals displayed surviving grafts predominantly confined to the striatum, as revealed by staining against the human specific neural cell adhesion protein, PSA-NCAM (Figure 4E–H). No evident tissue overgrowths were observed in any grafts, indicating that the implanted progenitors were sufficiently fate restricted in vitro prior to implantation. Volumetric assessment of the PSA-NCAM+ graft revealed that grafts in the presence of the GDNF-functionalized SAP hydrogel (Cells + SAP-shGDNF) were significantly larger (twofold) than cells in the absence or presence of SAP or sGDNF alone (Figure 4I). Total cells within the grafts, quantified using HNA immunolabeling, showed no significant difference between Cells, Cells + sGDNF, or Cells + SAP, indicating that the presence of the biomaterial had no impact on the overall survival of cells, nor their distribution (i.e., the hydrogel did not impede the migration and distribution of cells within the graft core). Commensurate with the increase in graft volume, cell grafts encapsulated in GDNF-functionalized scaffolds showed an increase (1.9-fold) in HNA+ cells, but no change in overall cell density (Figure 4J,K).

3.5. Tissue Specific Scaffolds Show In Vivo Biocompatibility and Are Vascularized by Host-Derived Endothelia

While short-term assessment of VM progenitors in the presence of the IKVAV SAP hydrogel revealed no significant change in the host inflammatory response compared to grafts of cells alone (Figure 2H,I), we more rigorously assessed the long-term biocompatibility of the hydrogel (inclusive of GDNF functionalization). Immunolabeling for astrocytes (GFAP) and microglia (CD11b) at 6 months after implantation showed no evident inflammatory response to the hydrogel. Compared to cell grafts alone (Cells), neither the presence of unfunctionalized or GDNF-functionalized SAPs increased GFAP or CD11b cell density, either at the graft–host interface (Figure S2A-G, Supporting Information) or at protracted distances from the graft core (data not shown).

TH+ cells and longer neurites. K–M) Representative pictures from VM primary culture with and without sGDNF or shGDNF-CM, illustrating increased TH+ DA neurons in the presence of GDNF, and N,P) longer neurites. Q) hPSC-derived VM progenitors, matured in the presence of GDNF (delivered directly to the media or via shGDNF-CM) showed enhanced viability and R) maturation into TH+ DA neurons compared to cultures lacking GDNF. S–U) Representative images TH+ DA neurons within differentiating hPSC-derived VM cultures in the absence and presence of GDNF. Data represent mean ± SEM. H,I,P) $n = 3$ independent cultures. *$p < 0.05$, **$p < 0.01$, and ***$p < 0.001$. Scale bars: B) 100 nm, K–M,S–U) 100 μm, and N–P) 25 μm.

ADVANCED
SCIENCE NEWS
www.advancedsciencenews.com

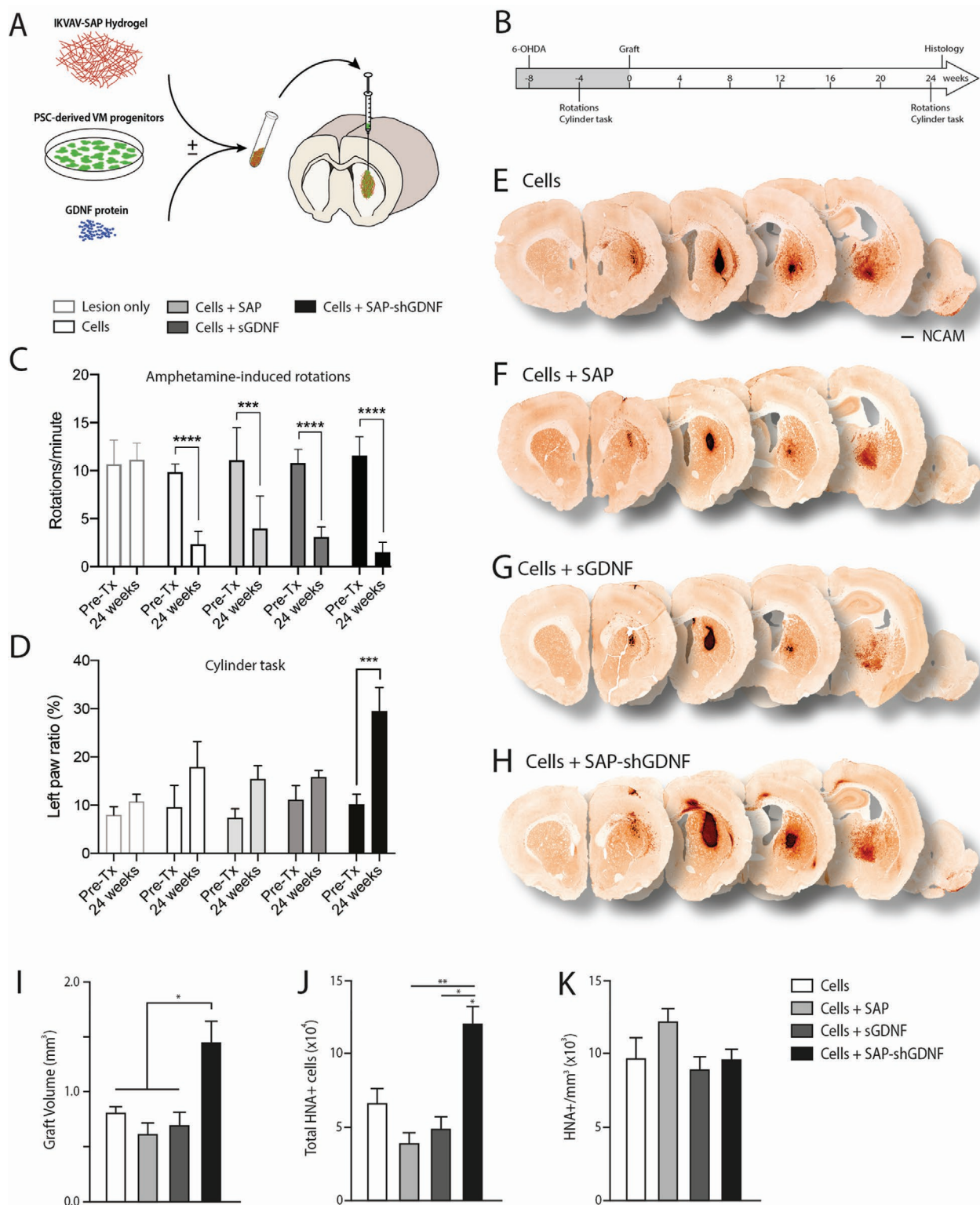ADVANCED
FUNCTIONAL
MATERIALS
www.afm-journal.de

Figure 4. Implantation of human ESC-derived VM progenitors together with a GDNF-functionalized tissue-specific scaffold improves motor function in Parkinsonian rats. A) Schematic of in vivo study design and B) timeline of surgical intervention and behavioral testing. C) All animals receiving a human PSC-derived VM progenitor cell graft showed significant correction of amphetamine-induced rotational asymmetry. D) Only animals receiving cell grafts in the presence of the GDNF-functionalized SAP scaffold (Cells + SAP-shGDNF) displayed a significant recovery in the cylinder task at 24 weeks after grafting. E–H) Representative photomicrographs of DA grafts confirmed graft survival as shown by PSA-NCAM staining after 24 weeks. I) Graft volumetric assessment by PSA-NCAM labeling revealed that grafts in the presence of the GDNF-functionalized SAP hydrogel were significantly larger compared to the other graft groups. J) A concomitant increase in the total number of HNA+ cells was observed in the Cells + SAP-shGDNFP group. K) SAP hydrogels did not alter the density of grafted cells after 24 weeks. Data represent mean ± SEM, $n = 6$–7 grafts per group. $^*p < 0.05$ and $^{**}p < 0.01$. Scale bar: E–G) 1 mm.

**ADVANCED
SCIENCE NEWS**

www.advancedsciencenews.com

**ADVANCED
FUNCTIONAL
MATERIALS**

www.afm-journal.de

Given that the inflammatory response may have subsided many months after the implantation, and that the death of DA progenitors occurs acutely during preparation of the tissue/cell suspension, or within days of implantation,[5a] in a separate cohort of animals, the density of GFAP immunoreactive astrocytes was assessed acutely (2 weeks) postimplantation. Similar to assessment at 6 months, the presence of the biomaterial imparted no inflammatory response above that observed in animals implanted with Cells alone (Figure S2H-J, Supporting Information).

Necessary for the survival of cells within large grafts is their proximity to a vascular supply. Staining against the rat endothelial cell antigen (RECA1+) and human collagen 1A1 (hCOL1A1) to identify host- or graft-derived vascular endothelial cells lining blood vessels, respectively, as well as HNA and GFP to demarcate the graft, revealed the presence of a modest vascular network within the grafts (Figure S3, Supporting Information). In alignment with other recent hPSC-derived VM grafts,[30] and unsurprising given the neural specification of the hPSCs in vitro and isolation of LMX1A-GFP VM neural progenitors prior to transplantation, the vasculature network within the grafts was not of graft origin (hCOL1A1+), but almost exclusively from infiltrating host endothelial cells (RECA1+) (Figure S3A,B, Supporting Information). Quantitative assessment revealed RECA1+ vessel density was less within the grafts compared to the host brain, with no difference observed between grafted groups (Figure S3C-H, Supporting Information), indicating that neither the biomaterial nor the GDNF influenced vascularization of the graft.

3.6. Functionalized Scaffolds Promote Survival of DA Neurons and Bias A9-Specification

Coimmunoreactivity for neuronal nuclei (NeuN+) and HNA+ revealed that approximately a third of the cells within all grafts adopted a mature neuronal phenotype, irrespective of the presence of the hydrogel or GDNF protein (**Figure 5**A–C). Necessary for these neural grafts to influence motor function is their capacity to form mature, TH-expressing DA neurons. As previously reported of LMX1A-GFP isolated progenitor grafts,[22] ≈7% of the total graft expressed coexpressed TH (TH+/HNA+). While the acute delivery of GDNF (Cells + sGDNF) or presence of the IKVAV SAP hydrogel (Cells + SAP) had no impact on TH+ cell number, grafts in the presence of the SAP scaffold, sustaining GDNF delivery (Cells + SAP-shGDNF), showed a 2.7-fold increase in TH+ cells (Figure 5D–H). This increase in DA neurons within the graft was over and above the increase in graft volume, with TH+ cell density notably elevated (Cells: 8.2 ± 1.4 TH+ mm^{-3}; Cells + SAP-shGDNF: 11.7 ± 1.9 TH+ mm^{-3}) (Figure 5I).

Importantly the presence of the hydrogel and/or GDNF had no impact on the capacity of the TH+ neurons within the grafts to acquire a mature fate, with >70% of all TH+ cells within the grafts showing GIRK2+ and/or Calbindin (CALB+) colocalization, indicative of A9-like SN and A10-like ventral tegmental area (VTA) DA neurons (Figure 5J). With A9-like DA neurons within grafts specifically responsible for underpinning the restoration of motor function,[8] more detailed assessment of the numbers and proportion of these phenotypes were determined.

A significant shift in TH+GIRK2+ A9 fated cells was observed in the presence of the SAP hydrogel (Cells: 1727 ± 114; Cells + SAP: 2878 ± 157; Cells + sGDNF: 2609 ± 148; Cells + SAP-shGDNF: 7014 ± 592). This increase in A9 fate acquisition was at the expense of A10-like identity, with a reciprocal decrease in TH+CALB+ cells (Cells: 750 ± 32; Cells + SAP: 349 ± 80; Cells + sGDNF, 637 ± 63; Cells + SAP-sh-GDNF: 1618 ± 157 TH+CALB+ cells) (Figure 5K,M,N). Assessment of the relative proportion of TH+ cells acquiring A9 or A10 fate revealed that this fate shift was specific to the presence of the SAP hydrogel, and not an additive effect of sustained GDNF, as both Cells + SAP and Cells + SAP-shGDNF showed a significant increase in the proportion of GIRK2+ cells (43% and 38%, respectively), compared to grafts of Cells alone (28%) (Figure 5L).

3.7. Functionalized Scaffolds Support the Integration of hPSC-Derived VM Graft

Next, the capacity of the grafted neurons to innervate the host striatum was assessed. Underpinning observed improvements in spontaneous motor function, only grafts in the presence of GDNF-functionalized scaffolds (Cells + SAP-shGDNF) showed a significant increase in density of graft-derived human PSA-NCAM+ fibers (**Figure 6**A,D,G). Within the grafts, comparable levels of TH labeling confirmed that the majority of the graft-derived innervation was dopaminergic (Figure 6B,E,H), as previously reported for human VM progenitor grafts.[6a] A more detailed assessment, specifically of the dopaminergic synapses within the dorsolateral striatum, revealed a significant (28%) increase in the density of puncta showing colocalization of TH and the presynaptic human protein synaptophysin (hSYP) (TH+hSYP+) in animals grafted with Cells + SAP-shGDNF compared to Cells alone (Figure 6C,F,I). Note that grafts of Cells alone (Cells) showed increased hSYP-immunoreactive puncta not colocalized with TH, indicative of non-DA synapses (Figure 6F, arrowheads).

3.8. Biochemical and Transcriptional Profiling Confirms Enhanced Functionality and Maturity of Grafts Supported by GDNF-Functionalized Scaffolds

With increased TH synaptogenesis observed, we subsequently assessed the ability of these grafts to release and utilize dopamine. HPLC confirmed extensive lesioning of the host midbrain dopamine system with striatal dopamine levels <5% of the intact brain in ungrafted 6OHDA mice at 6 months (**Figure 7**A). Human PSC-derived VM progenitor grafts significantly elevated striatal dopamine compared to Lesion only, with levels not effected by the presence of the hydrogel (Cells + SAP) or acute GDNF delivery (Cells + sGDNF). In contrast, and reflective of the improvement in sensorimotor function in the cylinder task, grafts supported by the functionalized SAP hydrogels (Cells + SAP-shGDNF, black bar) resulted in a 137% increase in dopamine levels compared to grafts of Cells alone, and 53.2% of the intact brain (Figure 7A,B).

The increase in striatal DA levels and observed functional recovery within Cells + SAP-shGDNF grafted animals was
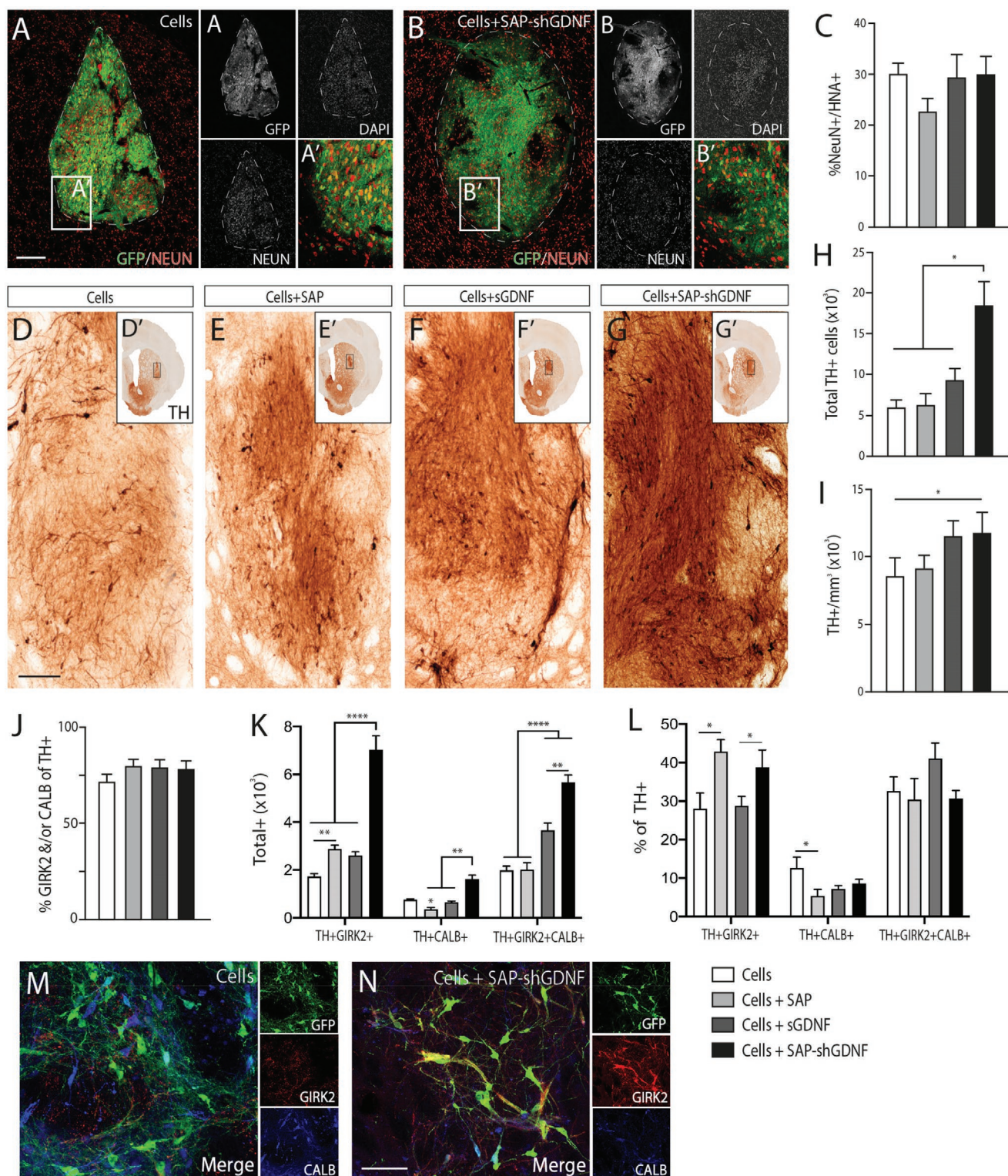
**ADVANCED
SCIENCE NEWS**
www.advancedsciencenews.com

**ADVANCED
FUNCTIONAL
MATERIALS**
www.afm-journal.de

Figure 5. Functionalized scaffolds increase graft size, DA neuron yield, and bias A9-specification. Representative pictures of NeuN+/HNA+ coexpression in a graft of A) Cells alone and B) Cells + SAP-shGDNF. C) Approximately a third of the cells within all grafts adopted a mature neuronal phenotype, irrespective of the presence of the hydrogel and/or GDNF. D–G) Representative photomicrographs of TH+ cells within grafts, at 24 weeks, showing that grafts in the presence of a GDNF-functionalized SAP scaffold had increased TH+ cells. H) Quantification of TH+ cells within the graft and I) density of TH+ cells. J) TH+ neruons within grafts (irrespective of the presence of SAP or GDNF) showed comparable maturation into GIRK2+ and/or CALB+ expressing cells. K) Grafts in the presence of a GDNF-functionalized SAP scaffold showed an increase in TH+/GIRK2+, TH+/CALB+, and TH+/GIRK2+/CALB+ cells, indicative of DA graft survival. L) Expressed as a proportion of TH+ cells, only grafts in the presence of the tissue-specific

ADVANCED
SCIENCE NEWS
www.advancedsciencenews.com

ADVANCED
FUNCTIONAL
MATERIALS
www.afm-journal.de
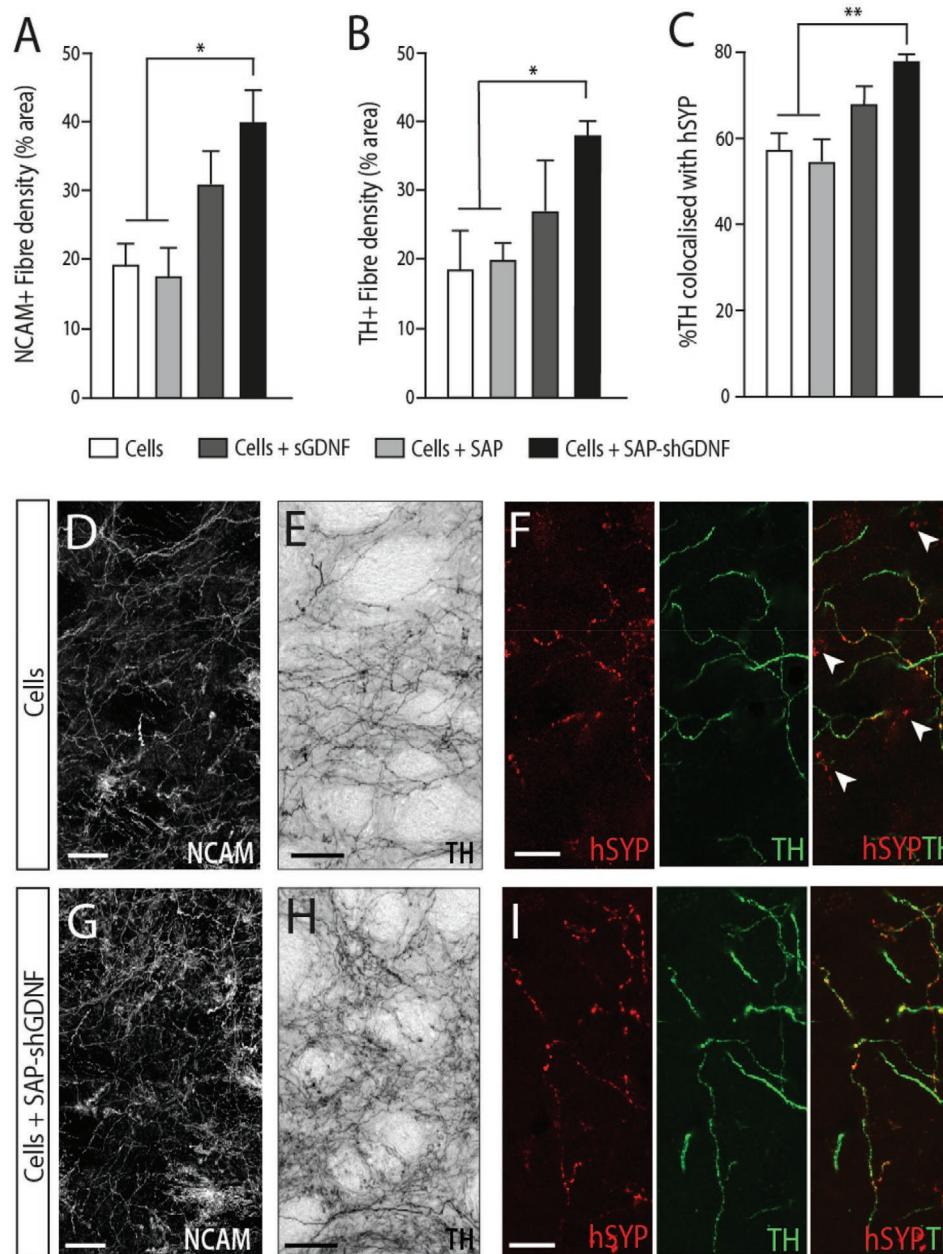
Figure 6. GDNF-functionalized hydrogels enhance graft plasticity and dopaminergic synapse formation. A) Quantification of graft-derived human NCAM fiber density within the host striatum and B) tyrosine hydroxylase fiber density. C) Quantitative assessment of the proportion of TH-immunoreactive puncta colocalized with hSYP within the host striatum, indicating that GDNF-functionalized scaffolds promoted maturation of DA synapses. D,G) Representative photomicrographs of NCAM-labeled graft fibers within the striatum of an animal grafted with cells alone, or cells + SAP-shGDNF. E,H) Example images of TH+ fiber density in a graft of Cells alone, and in the presence of the GDNF shear-encapsulated hydrogel. F) Photomicrographs showing hSYP and TH labeling (plus merged images) taken from the host striatum of a rat grafted with Cells and I) Cells + SAP-shGDNF; white arrows represent hSYP+ puncta that do not colocalize with TH+ fibers. Data represent mean ± SEM, $n = 6$–7 grafts per group. $^*p < 0.05$ and $^{**}p < 0.01$. Scale bars: D,E,G,H) 100 μm and F,I) 25 μm.

further verified by activation of postsynaptic striatal neurons. Following acute amphetamine administration, the upregulation of the intermediate early response gene, cFos, within DARPP32+ medium spiny neurons of the striatum has been shown to

be an indirect measure of DA release, including from grafted rodent and human DA neurons.[16,31] Reflective of striatal dopamine depletion, ungrafted 6OHDA lesioned animals showed a significant reduction in the density of cFos-immunoreactive

IKVAV SAP hydrogel showed a significant increase in the percentage of TH+/GIRK2+ (A9-like DA neurons), at the expense of TH+/CALB+ (A10-like). M,N) Representative photomicrographs of GIRK2, Calbinidn (CALB+), and TH+ cells within a Cells or Cells + SAP graft. Data represent mean ± SEM, $n = 6$–7 grafts per group. $^*p < 0.05$, $^{**}p < 0.01$, and $^{****}p < 0.0001$. Scale bar: A,B,D–G) 200 μm and L,M) 100 μm.
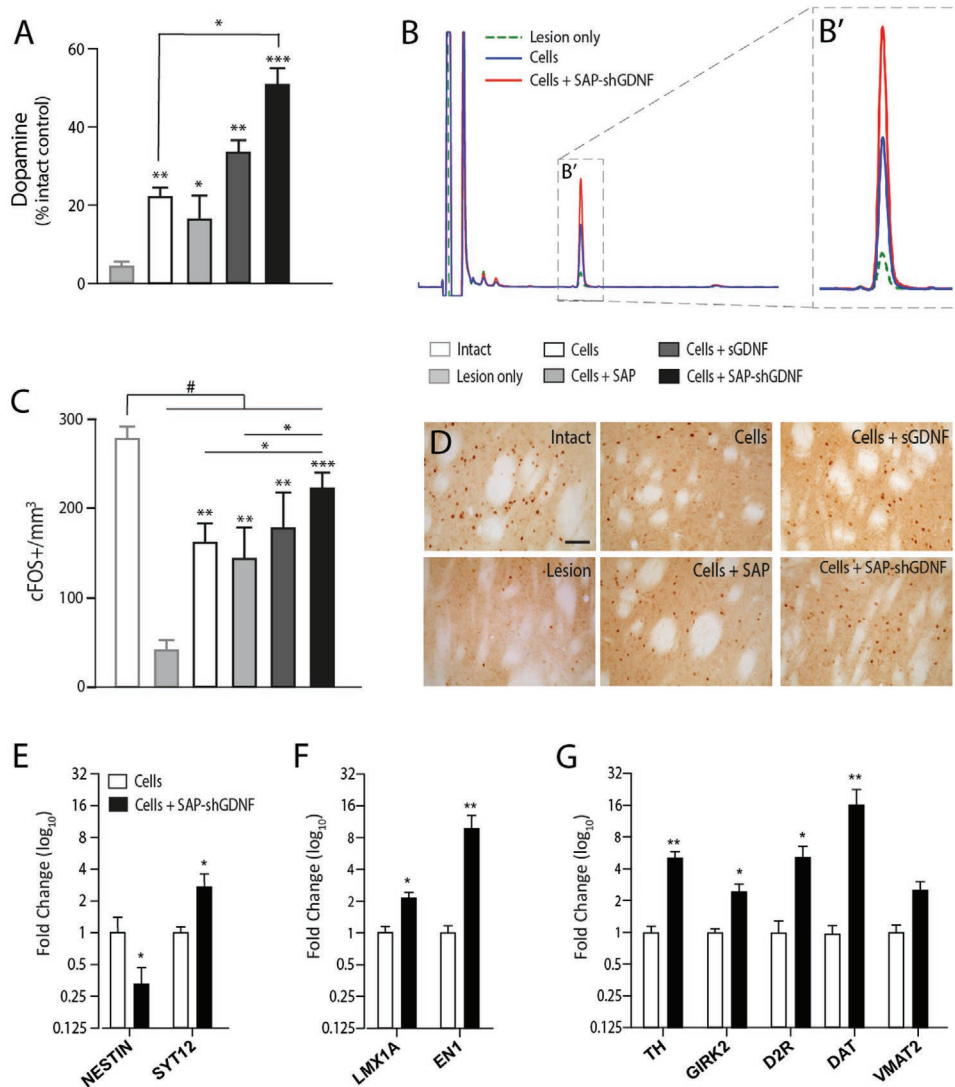
Figure 7. Biochemical and transcriptional profiling confirmed increased dopamine levels, functionality, and maturity of VM grafts in the presence of the GDNF-functionalized hydrogel. A) HPLC confirmed extensive ablation of the host striatal dopamine levels, an effect that was partially restored by hPSC-derived VM DA grafting, and further elevated (2.3-fold) by the presence of the GDNF-functionalized hydrogel. B) Overlaid representative HPLC chromatography traces illustrating dopamine levels within the striatum of lesioned mouse (green), and animals receiving a cell graft in the absence (blue) and presence of the SAP-shGDNF hydrogel (red). B') Enlargement of the DA peak. C) Quantification of c-FOS+ cells within the host brain revealed significant increases in activated cells in the dorsolateral striatum of grafted animals, irrespective of the presence of GDNF and or the SAP hydrogel. D) Representative photomicrographs of cFOS-labeling in the host brain of control (intact), lesion, and grafted (±SAP ± GDNF) animals. E) Species-specific primers for neural-associated genes Nestin and synaptotagmin12 (SYT12) confirmed increased maturation of grafts in the presence of the GDNF-functionalized SAP gel. F) Graft expression of early ventral midbrain progenitor transgenes LMX1A and Engrailed-1 (EN1), as well as G) late expressed VM DA genes (TH, GIRK2, D2R, DAT, and VMAT) confirmed the increased DA neuron yield, maturity, and functionality from hPSC-derived VM progenitor grafts in the presence of SAP-shGDNF hydrogel. Data represent mean ± SEM; C) $n = 5-6$ animals per group; A,E–G) $n = 4-5$ animals per group. *$p < 0.05$ and **$p < 0.01$. Scale bar: D) 100 μm.

cells within the dorsolateral striatum compared to intact control animals (Figure 7C). Comparatively, all grafted animals showed a significant increase in the density of cFos+ cells compared to the Lesion only group, effects that were further, and significantly, accentuated by the presence of the SAP-shGDNF hydrogel (Cells + SAP-shGDNF, black bar) (Figure 7C,D).

Finally, transcriptional profiling confirmed the observed enhanced maturity and functionality of VM progenitor grafts in the presence of the functionalized SAP hydrogels (Cells + SAP-shGDNF). Expression of the neuroectodermal stem cell

marker, NESTIN, was significantly reduced in grafts of Cells + SAP-shGDNF compared to Cells alone, while the presynaptic protein, Synaptotagmin 12 (SYT12) was significantly upregulated, reflective of neuronal maturation as observed in development[32] (Figure 7E). Specific examination of the dopamine population within grafts revealed significant upregulation of early VM determinant genes *LMX1A* and Engrailed-1 (*EN1*, also critical for VM DA survival) within Cells + SAP-shGDNF grafts (Figure 7F), as well as later expressed genes involved in the maturation and functionality of the DA neuron and synapse

including *TH*, *GIRK2* (specific to the A9 DA neurons), *D2R* (the D2 DA autoreceptor expressed on the presynaptic terminal that regulate DA release and firing of action potentials), the dopamine transporter (*DAT*, responsible for DA reuptake), as well as the vesicular monoamine transporter (*VMAT2*, responsible for the recycling and reuptake of DA into the synaptic vesicles within DA terminals) (Figure 7G).

4. Discussion

Biomaterials have the capacity to significantly improve cell transplantation for neural repair and have been examined most extensively in their capacity to support cell grafts after stroke (see reviews – (Bruggeman et al., 2019; Jendelova et al., 2016). Recently we demonstrated the benefits of functionalised natural and synthetic polymers, which recapitulate structural and biochemical elements of the extracellular matrix, to promote the survival, differentiation and functional integration of rodent fetal tissue grafts in models of Parkinson's disease.[12a,b,33] With hPSC now rapidly advancing into the clinic for cell replacement therapy in PD patients, there is an evident need to understand how biomaterials may also support and improve these graft outcomes. Recent efforts, utilizing functionalized hyaluronic acid hydrogels, have made some attempt to support hPSC-derived DA progenitors/neurons during transplantation, yet showed notably small grafts with limited integration into the host tissue and functionality below standard levels.[34] Here, we fabricated and assessed a series of functionalized and nonfunctionalized peptide-based hydrogels, identifying a neural tissue-specific laminin mimetic peptide capable of supporting VM neural progenitors in vivo. Through shear encapsulation, this IKVAV SAP hydrogel could be functionalized to sustain presentation of the neurotrophic factor GDNF, improving long-term graft outcomes. In animals receiving these cell grafts supported by the GDNF-functionalized hydrogel, both induced and spontaneous motor deficits were ameliorated. Underpinning these behavioral improvements were increases in DA neurons (and more specifically the number and proportion of A9-like DA cells), as well as their capacity to innervate appropriate host target nuclei and DA release.

Anoikis, a form of programmed cell death that occurs when anchorage-dependent cells are detached from their surrounding extracellular matrix, affects donor cells during their harvest from in vitro cultures (or dissociation of fetal tissue) as well as acutely post implantation if the donor cells fail to form new, local adhesions.[35] While a range of soft hydrogels that gel in situ have been trialed to protect cells against shear forces during implantation and rebuild de novo tissue where necessary, there remains a requirement for engineered scaffolds to provide cell adhesive matrix in situ.[36] In this regard, the SAP-based hydrogel employed here, presenting the cell adhesive epitope (IKVAV) for laminin, provided a tissue-specific biomimetic of the native neural ECM. In vitro, this functional epitope has been shown to promote neuronal adhesion and survival with greater efficiency than laminin protein itself, due to its high density of signal presented to the surface.[37] In vivo, IKVAV-presenting SAP hydrogels have also been shown to promote the survival of hPSC-derived cortical progenitors,[14–15] yet

surprisingly had no comparable impact on VM progenitors, as highlighted by acute assessment of grafts at 6 weeks. Such observations suggest that further study into region-specific ECM differences may aid design of future hydrogels.

In addition to their adhesive properties, ECM proteins (including laminins) contribute to stem cell maintenance, differentiation and plasticity[38]—roles that have been confirmed using IKVAV peptides for cultured and transplanted cortical progenitors.[14–15] Surprisingly, within the present findings, the IKVAV SAP hydrogel had no impact on the maturation of VM progenitors into postmitotic neurons or acquisition of TH+ DA identity within grafts, yet importantly biased A9 specification, at the expense A10 DA neurons. Likely underpinning these disparate outcomes is the complexity of the laminin family of proteins. Laminins are heterotrimeric proteins that contain α-, β-, and γ-chains, with the employed nomenclature describing the chains present (e.g., laminin-521 comprising of a α5, β2, and a γ1 subunit)—with a total of 16 laminin trimers identified to date in mammals. Of relevance, recent success in the directed differentiation of hPSC into VM DA progenitors/neurons has been underpinned by the culturing of cells on various laminin substrates, identifying four specific laminins in this capacity (Lam-111, Lam-421, Lam-511, and Lam-521).[2c,6b,29a] With hPSC-DA differentiation protocols varying between research groups, differing success with different laminins have been observed, indicating that identification of the necessary and optimal subunits remains to be determined and/or the existence of redundant roles. Further insight can also be gained from recent deep-sequencing analysis of laminin subchain expression within the developing mouse and human midbrain.[10c,39] While here we demonstrate benefits of the α1 subunit in A9 DA specification and show inferior grafting outcomes in the presence of the β1 subunit (YIGSR), further studies assessing alternative laminin subunit (and/or the associated integrin transmembrane receptor) will be required to determine the optimal subunit s^{-1} for inclusion into fabricated SAP hydrogels aimed at supporting hPSC-derived VM grafts for PD.

While the IKVAV peptide sequence had no effect on DA survival or differentiation in the current context, the increase in A9 specification observed here (both the total number of GIRK2+ cells and their proportion of the DA neuronal population) provides the first evidence, to our knowledge, of selectively enriching for this subpopulation of DA neurons within human PSC-derived grafts. Acknowledging the specific requirement for this subpopulation of DA neurons to restore motor deficits following transplantation,[8] such an enrichment suggests that the implantation of fewer cells, with more targeted function, may be a feasible prospect for future clinical application.

Growth factor deprivation of progenitors isolated from the developing embryo or in vitro cultures is a major contributor to cell death during acute graft integration. Such observations have justified a large body of work focused on reintroducing GDNF into the adult brain to support DA progenitor grafts (see review in ref. [40]). In addition to the impact on graft survival, GDNF is involved in DA plasticity and maturation. In the present study, acute delivery of GDNF failed to influence survival or plasticity, a likely consequence of insufficient dose and/or duration of delivery, noting that previous studies required repeated GDNF doses over weeks,[41] or continual

infusion[42] in order to influence fetal graft outcomes. In more recent years, viral delivery approaches have been employed to sustain GDNF level—targeted at slowing PD progression[43] and supporting grafts.[16,17b,40,44] However, a recognized challenge of this approach has been the inability to silence the transgene after graft integration, which can result in aberrant axonal growth and downregulation of DA-associated genes in host and hPSC-derived DA grafts.[16–17] Consistent with our efforts to support rodent fetal grafts,[12a,b] here, we show prolonged delivery of GDNF from IKVAV-SAP promoted the survival and plasticity of hPSC-derived VM progenitor grafts. In vitro, we showed an initial burst release of GDNF, followed by a delayed and sustained delivery beyond 28 days, with this biphasic delivery likely underpinning initial progenitor survival, and subsequent integration. The modest, but significant, effects on graft plasticity suggest that higher concentrations of GDNF, and/or the incorporation of other DA axonal growth promoting proteins, such as Wnt5a,[24] may enhance graft plasticity and functional integration. Added to this, future studies should endeavor to explore whether biomaterials can support the survival and integration of homotopically transplanted cells (implanted back into the VM), as well as sustain GDNF delivery from functionalized hydrogels, simultaneously implanted into the target striatum, aimed at encouraging reconstruction of the nigrostriatal pathway that degenerates in PD. Such future studies should additionally seek to perform more rigorous behavioral testing in order to assess the full potential of these biomaterial-supported transplants to reverse motor deficits in Parkinsonian models.

Vascularization of solid tissue grafts is critical for their survival, yet surprisingly little attention has been paid to the vessel network within fetal or human PSC-derived VM progenitor grafts. We provide here the first characterization of blood vessels within VM grafts, showing the presence of organized host-derived endothelial cells. These observations highlight the permissiveness of the hydrogel to enable not only the outgrowth of axonal processes from the graft, but additionally the infiltration of host-derived endothelial cells into the graft core. Evident, however, was the inferior density and maturation of the vessel network across all graft conditions compared to the host tissue, suggesting that delivery of additional trophic cues, targeted at promoting angiogenesis, may improve vessel formation and consequently influence graft survival and/or maturation—as has been observed following hydrogel-based delivery of BDNF into human PSC-derived neural grafts in stroke.[15]

Taken together, these findings provide the first substantiated evidence for a functionalized, tissue-specific hydrogel to improve the survival, differentiation, and integration of human PSC-derived DA progenitor grafts in an animal model of PD. These findings highlight that additional efforts, incorporating functionalized biomaterials to influence the donor cells and host tissue should be considered as the field moves toward the clinic. Here, we present findings for a laminin α1 subchain peptide hydrogel presenting GDNF, providing the impetus for greater attention to ECM-related and growth factor related strategies. Further studies targeting additional/alternative proteins for neuroprotection, plasticity, and vascularization, are necessary to ensure maximal functional benefits can be obtained from grafted progenitors—targeted not only for cell replacement therapy in PD, but other conditions where cell transplantation presents a therapeutically viable option.

Supporting Information

Supporting Information is available from the Wiley Online Library or from the author.

Conflict of Interest

The authors declare no conflict of interest.

Data Availability Statement

The data that support the findings of this study are openly available in figshare at https://doi.org/10.6084/m9.figshare.15057570.v1.

[1] R. A. Barker, M. Parmar, A. Kirkeby, A. Bjorklund, L. Thompson, P. Brundin, *J. Parkinson's Dis.* **2016**, *6*, 57.
[2] a) A. Kirkeby, S. Grealish, D. A. Wolf, J. Nelander, J. Wood, M. Lundblad, O. Lindvall, M. Parmar, *Cell Rep.* **2012**, *1*, 703; b) S. Kriks, J. W. Shim, J. Piao, Y. M. Ganat, D. R. Wakeman, Z. Xie, L. Carrillo-Reid, G. Auyeung, C. Antonacci, A. Buch, L. Yang,

**ADVANCED
SCIENCE NEWS**

www.advancedsciencenews.com

**ADVANCED
FUNCTIONAL
MATERIALS**

www.afm-journal.de

M. F. Beal, D. J. Surmeier, J. H. Kordower, V. Tabar, L. Studer, *Nature* **2011**, *480*, 547; c) J. C. Niclis, C. W. Gantner, W. F. Alsanie, S. J. McDougall, C. R. Bye, A. G. Elefanty, E. G. Stanley, J. M. Haynes, C. W. Pouton, L. H. Thompson, C. L. Parish, *Stem Cells Transl. Med.* **2017**, *6*, 937.

[3] S. Grealish, E. Diguet, A. Kirkeby, B. Mattsson, A. Heuer, Y. Bramoulle, N. Van Camp, A. L. Perrier, P. Hantraye, A. Bjorklund, M. Parmar, *Cell Stem Cell* **2014**, *15*, 653.

[4] R. A. Barker, M. Parmar, L. Studer, J. Takahashi, *Cell Stem Cell* **2017**, *21*, 569.

[5] a) R. F. Castilho, O. Hansson, P. Brundin, *Prog. Brain Res.* **2000**, *127*, 203; b) P. Hagell, P. Brundin, *J. Neuropathol. Exp. Neurol.* **2001**, *60*, 741.

[6] a) J. C. Niclis, C. W. Gantner, C. P. J. Hunt, J. A. Kauhausen, J. C. Durnall, J. M. Haynes, C. W. Pouton, C. L. Parish, L. H. Thompson, *Stem Cell Rep.* **2017**, *9*, 868; b) D. Doi, B. Samata, M. Katsukawa, T. Kikuchi, A. Morizane, Y. Ono, K. Sekiguchi, M. Nakagawa, M. Parmar, J. Takahashi, *Stem Cell Rep.* **2014**, *2*, 337; c) B. Samata, D. Doi, K. Nishimura, T. Kikuchi, A. Watanabe, Y. Sakamoto, J. Kakuta, Y. Ono, J. Takahashi, *Nat. Commun.* **2016**, *7*, 13097.

[7] N. Moriarty, C. L. Parish, E. Dowd, *Eur. J. Neurosci.* **2019**, *49*, 472.

[8] S. Grealish, M. E. Jonsson, M. Li, D. Kirik, A. Bjorklund, L. H. Thompson, *Brain* **2010**, *133*, 482.

[9] D. Kirik, C. Winkler, A. Bjorklund, *J. Neurosci.* **2001**, *21*, 2889.

[10] a) C. R. Bye, W. Alsanie, C. L. Parish, L. H. Thompson, *J. Neurosci.* **2019**, *39*, 6656; b) W. F. Alsanie, V. Penna, M. Schachner, L. H. Thompson, C. L. Parish, *Sci. Rep.* **2017**, *7*, 9368; c) D. Zhang, S. Yang, E. M. Toledo, D. Gyllborg, C. Salto, J. C. Villaescusa, E. Arenas, *Sci. Signaling* **2017**, *10*, eaal4165.

[11] a) K. F. Bruggeman, N. Moriarty, E. Dowd, D. R. Nisbet, C. L. Parish, *Br. J. Pharmacol.* **2019**, *176*, 355; b) P. Jendelova, S. Kubinova, I. Sandvig, S. Erceg, A. Sandvig, E. Sykova, *Expert Opin. Biol. Ther.* **2016**, *16*, 43.

[12] a) T. Y. Wang, K. F. Bruggeman, J. A. Kauhausen, A. L. Rodriguez, D. R. Nisbet, C. L. Parish, *Biomaterials* **2016**, *74*, 89; b) N. Moriarty, A. Pandit, E. Dowd, *Sci. Rep.* **2017**, *7*, 16033; c) N. Moriarty, C. L. Parish, E. Dowd, *Eur. J. Neurosci.* **2018**, *49*, 472.

[13] Y. Wang, X. He, K. F. Bruggeman, B. Gayen, A. Tricoli, W. M. Lee, R. J. Williams, D. R. Nisbet, *Adv. Funct. Mater.* **2020**, *30*, 1900390.

[14] F. A. Somaa, T. Y. Wang, J. C. Niclis, K. F. Bruggeman, J. A. Kauhausen, H. Guo, S. McDougall, R. J. Williams, D. R. Nisbet, L. H. Thompson, C. L. Parish, *Cell Rep.* **2017**, *20*, 1964.

[15] D. R. Nisbet, T. Y. Wang, K. F. Bruggeman, J. C. Niclis, F. A. Somaa, V. Penna, C. P. Hunt, Y. Wang, J. A. Kauhausen, R. J. Williams, L. H. Thompson, C. L. Parish, *Adv. Biosyst.* **2018**, *2*, 1800113.

[16] C. W. Gantner, I. R. de Luzy, J. A. Kauhausen, N. Moriarty, J. C. Niclis, C. R. Bye, V. Penna, C. P. J. Hunt, C. M. Ermine, C. W. Pouton, D. Kirik, L. H. Thompson, C. L. Parish, *Cell Stem Cell* **2020**, *26*, 511.

[17] a) C. Winkler, B. Georgievska, T. Carlsson, B. Lacar, D. Kirik, *Neuroscience* **2006**, *141*, 521; b) J. D. Elsworth, D. E. Redmond Jr., C. Leranth, K. B. Bjugstad, J. R. SladekJr., T. J. Collier, S. B. Foti, R. J. Samulski, K. P. Vives, R. H. Roth, *Exp. Neurol.* **2008**, *211*, 252.

[18] A. L. Rodriguez, C. L. Parish, D. R. Nisbet, R. J. Williams, *Soft Matter* **2013**, *9*, 3915.

[19] a) K. F. Bruggeman, A. L. Rodriguez, C. L. Parish, R. J. Williams, D. R. Nisbet, *Nanotechnology* **2016**, *27*, 385102; b) K. F. Bruggeman, Y. Wang, F. L. Maclean, C. L. Parish, R. J. Williams, D. R. Nisbet, *Nanoscale* **2017**, *9*, 13661; c) K. F. Bruggeman, R. J. Williams, D. R. Nisbet, *Adv. Healthcare Mater.* **2018**, *7*, 1700836; d) F. L. Maclean, G. M. Ims, M. K. Horne, R. J. Williams, D. R. Nisbet, *Adv. Mater.* **2018**, *30*, 1805209.

[20] T. Y. Wang, K. A. Bruggeman, R. K. Sheean, B. J. Turner, D. R. Nisbet, C. L. Parish, *J. Biol. Chem.* **2014**, *289*, 15044.

[21] B. D. Blakely, C. R. Bye, C. V. Fernando, M. K. Horne, M. L. Macheda, S. A. Stacker, E. Arenas, C. L. Parish, *PLoS One* **2011**, *6*, e18373.

[22] I. R. de Luzy, J. C. Niclis, C. W. Gantner, J. A. Kauhausen, C. P. J. Hunt, C. Ermine, C. W. Pouton, L. H. Thompson, C. L. Parish, *J. Neurosci.* **2019**, *39*, 9521.

[23] A. L. Rodriguez, T. Y. Wang, K. F. Bruggeman, C. C. Horgan, R. Li, R. J. Williams, C. L. Parish, D. R. Nisbet, *J. Mater. Chem. B* **2014**, *2*, 7771.

[24] C. L. Parish, G. Castelo-Branco, N. Rawal, J. Tonnesen, A. T. Sorensen, C. Salto, M. Kokaia, O. Lindvall, E. Arenas, *J. Clin. Invest.* **2008**, *118*, 149.

[25] C. R. Bye, V. Penna, I. R. de Luzy, C. W. Gantner, C. P. J. Hunt, L. H. Thompson, C. L. Parish, *Stem Cell Rep.* **2019**, *13*, 877.

[26] J. B. Matson, S. I. Stupp, *Chem. Commun.* **2012**, *48*, 26.

[27] J. Weickenmeier, M. Kurt, E. Ozkaya, R. de Rooij, T. C. Ovaert, R. L. Ehman, K. Butts Pauly, E. Kuhl, *J. Mech. Behav. Biomed. Mater.* **2018**, *84*, 88.

[28] C. W. Gantner, A. Cota-Coronado, L. H. Thompson, C. L. Parish, *STAR Protoc.* **2020**, *1*, 100065.

[29] a) A. Kirkeby, S. Nolbrant, K. Tiklova, A. Heuer, N. Kee, T. Cardoso, D. R. Ottosson, M. J. Lelos, P. Rifes, S. B. Dunnett, S. Grealish, T. Perlmann, M. Parmar, *Cell Stem Cell* **2017**, *20*, 135; b) I. R. de Luzy, K. C. L. Law, N. Moriarty, C. P. J. Hunt, J. C. Durnall, L. H. Thompson, A. Nagy, C. L. Parish, *Nat. Commun.* **2021**, *12*, 3275.

[30] T. W. Kim, J. Piao, S. Y. Koo, S. Kriks, S. Y. Chung, D. Betel, N. D. Socci, S. J. Choi, S. Zabierowski, B. N. Dubose, E. J. Hill, E. V. Mosharov, S. Irion, M. J. Tomishima, V. Tabar, L. Studer, *Cell Stem Cell* **2021**, *28*, 343.

[31] M. A. Cenci, P. Kalen, R. J. Mandel, K. Wictorin, A. Bjorklund, *Neuroscience* **1992**, *46*, 943.

[32] C. Wiese, A. Rolletschek, G. Kania, P. Blyszczuk, K. V. Tarasov, Y. Tarasova, R. P. Wersto, K. R. Boheler, A. M. Wobus, *Cell. Mol. Life Sci.* **2004**, *61*, 2510.

[33] a) N. Moriarty, S. Cabre, V. Alamilla, A. Pandit, E. Dowd, *Eur. J. Neurosci.* **2018**, *49*, 487; b) A. L. Rodriguez, K. F. Bruggeman, Y. Wang, T. Y. Wang, R. J. Williams, C. L. Parish, D. R. Nisbet, *J. Tissue Eng. Regener. Med.* **2018**, *12*, e1571.

[34] a) M. M. Adil, A. T. Rao, G. N. Ramadoss, N. E. Chernavsky, R. U. Kulkarni, E. W. Miller, S. Kumar, D. V. Schaffer, *Adv. Funct. Mater.* **2018**, *28*, 1804144; b) M. M. Adil, T. Vazin, B. Ananthanarayanan, G. M. C. Rodrigues, A. T. Rao, R. U. Kulkarni, E. W. Miller, S. Kumar, D. V. Schaffer, *Biomaterials* **2017**, *136*, 1.

[35] N. Moriarty, E. Dowd, *Neural Regener. Res.* **2018**, *13*, 1187.

[36] B. Newland, P. B. Welzel, H. Newland, C. Renneberg, P. Kolar, M. Tsurkan, A. Rosser, U. Freudenberg, C. Werner, *Small* **2015**, *11*, 5047.

[37] G. A. Silva, C. Czeisler, K. L. Niece, E. Beniash, D. A. Harrington, J. A. Kessler, S. I. Stupp, *Science* **2004**, *303*, 1352.

[38] U. Theocharidis, K. Long, C. ffrench-Constant, A. Faissner, *Prog. Brain Res.* **2014**, *214*, 3.

[39] a) G. La Manno, D. Gyllborg, S. Codeluppi, K. Nishimura, C. Salto, A. Zeisel, L. E. Borm, S. R. W. Stott, E. M. Toledo, J. C. Villaescusa, P. Lonnerberg, J. Ryge, R. A. Barker, E. Arenas, S. Linnarsson, *Cell* **2016**, *167*, 566; b) M. Ahmed, L. N. Marziali, E. Arenas, M. L. Feltri, C. ffrench-Constant, *Development* **2019**, *146*, dev172668.

[40] K. Farrell, R. A. Barker, *Degener. Neurol. Neuromuscular Dis.* **2012**, *2*, 79.

[41] C. Rosenblad, A. Martinez-Serrano, A. Bjorklund, *Neuroscience* **1996**, *75*, 979.

[42] D. M. Yurek, *Exp. Neurol.* **1998**, *153*, 195.

[43] D. Kirik, E. Cederfjall, G. Halliday, A. Petersen, *Neurobiol. Dis.* **2017**, *97*, 179.

[44] J. Kauhausen, L. H. Thompson, C. L. Parish, *J. Physiol.* **2013**, *591*, 77.